

Chain-of-Restoration: Multi-Task Image Restoration Models are Zero-Shot Step-by-Step Universal Image Restorers

Jin Cao

Xi'an Jiaotong University

2213315515@stu.xjtu.edu.cn

Deyu Meng

Xi'an Jiaotong University

dymeng@mail.xjtu.edu.cn

Xiangyong Cao*

Xi'an Jiaotong University

caoxiangyong@mail.xjtu.edu.cn

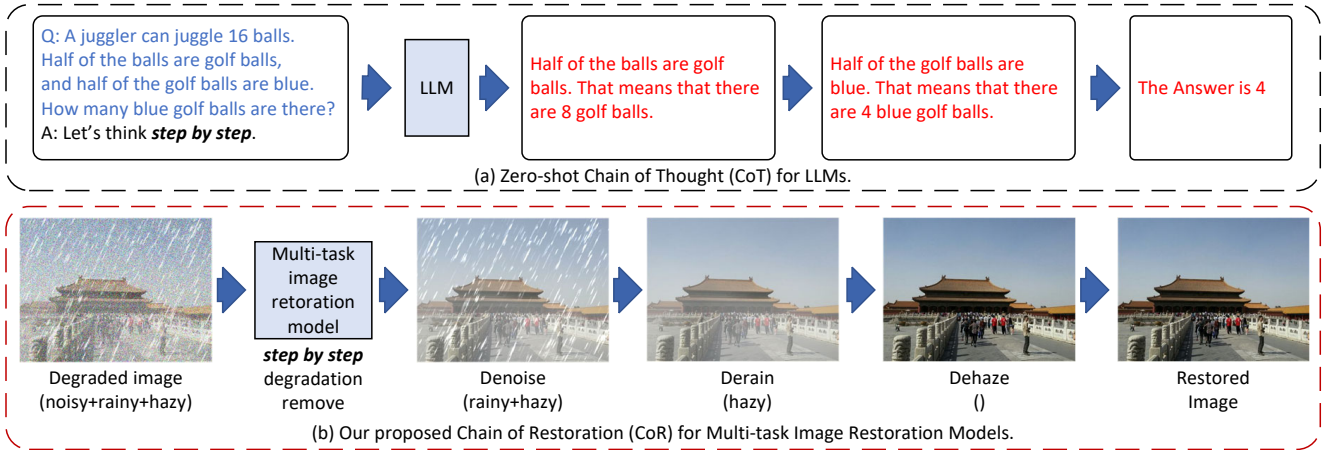


Figure 1. Comparison of CoT and CoR. (a) Zero-Shot CoT for LLMs. The core idea of CoT is to ask the LLM to response to break down the question into smaller components and solve them step by step. (b) Our proposed CoR. We take the composite degradation as combination of multiple degradation bases. Using multi-task models that are trained on these bases, we ask the model to remove the composite degradation step by step. In this paper, "multi-task model" refers to any image restoration model trained on more than one degradations.

Abstract

Despite previous works typically targeting isolated degradation types, recent research has increasingly focused on addressing composite degradations which involve a complex interplay of multiple different isolated degradations. Recognizing the challenges posed by the exponential number of possible degradation combinations, we propose Universal Image Restoration (UIR), a new task setting that requires models to be trained on a set of degradation bases and then remove any degradation that these bases can potentially compose in a zero-shot manner. Inspired by the Chain-of-Thought which prompts LLMs to address problems step-by-step, we propose the Chain-of-Restoration (CoR), which instructs models to step-by-step remove unknown composite degradations. By integrating a simple Degradation Discriminator into pre-trained multi-task models, CoR facilitates the process where models remove one degradation basis per step, continuing this process until the image is fully restored from the unknown composite degradation. Extensive

experiments show that CoR significantly improves model performance in removing composite degradations, achieving results comparable to or surpassing those of State-of-The-Art (SoTA) methods trained on all degradations. The code will be released [at this url](#).

1. Introduction

Image restoration plays a crucial role in the retrieval of high-fidelity imagery from corrupted sources and is extensively applied across various fields, including autonomous navigation, medical imaging, and surveillance systems. Considerable progress has been made in addressing isolated degradation scenarios by a One-to-One single-task model (Fig. 2a) [6, 10, 11, 13, 23, 37, 44, 60, 66, 67], such as low-light conditions [24, 40, 62, 63, 74], haze [22, 27, 51, 54, 72], rain [9, 18, 20, 31, 42], noise [16, 33, 55, 69, 70] and snow [7, 8, 12, 52, 58]. Despite their remarkable achievements in specific contexts, real-world conditions often involve unpredictable and variable degradations, posing significant challenges to single-task methods [36].

To overcome the limitations of One-to-One methods,

*Corresponding Author

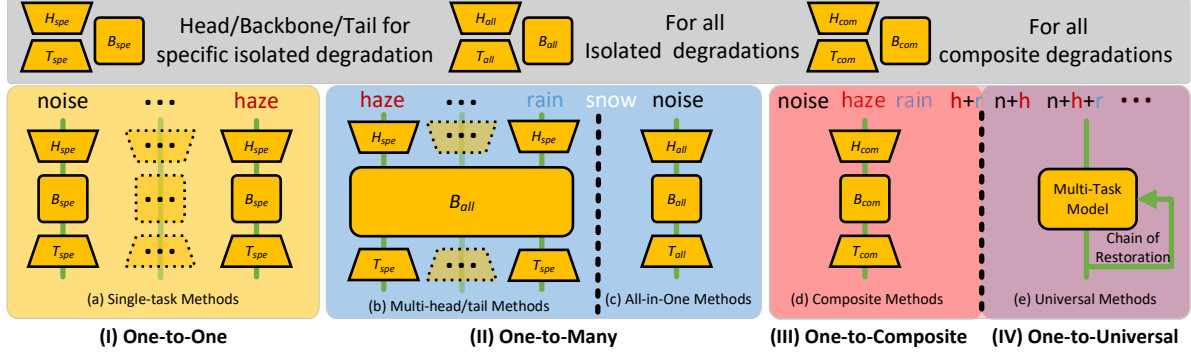


Figure 2. Comparison of task settings and classification of models in previous image restoration works. **(I) One-to-One:** In this setting, models are trained on a isolated degradation and tested on it. **(II) One-to-Many:** In this setting, models are trained on multiple isolated degradations simultaneously and tested on them simultaneously. **(III) One-to-Composite:** In this setting, models are trained on multiple isolated degradations and composite degradations simultaneously and tested on them simultaneously. **(IV) One-to-Universal:** In this setting, models are trained on a set of base degradations simultaneously and tested on combinations of these degradations.

there is an increasing need for versatile One-to-Many image restoration techniques that can efficiently handle a variety of degradations within a unified and adaptable framework. Initially, approaches with multiple heads or tails have been introduced [4, 26, 36, 59]. These techniques equip distinct heads or tails for each specific type of degradation, leveraging a common backbone for processing all degradations, as shown in Fig. 2b. Nonetheless, they necessitate extra parameters for each degradation task and rely on prior knowledge of the degradation type to select the appropriate head or tail, which may not always be feasible. Consequently, recent research has shifted towards All-in-One image restoration methods [3, 8, 35, 48, 49, 56, 57], employing a single blind model to manage all isolated degradations, as depicted in Fig. 2c. While these methods accomplish the blind image restoration, they are primarily designed for isolated degradation scenarios and do not fully address the intricate interplay that emerges when multiple degradation factors concurrently impact a single image.

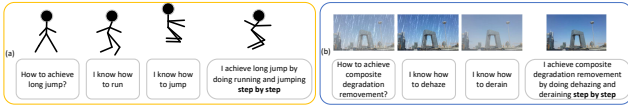


Figure 3. (a) To master long jump, the only requirements are knowing how to run and jump, executed step by step. (b) For an image degraded by both rain and haze, restoring it requires only a model capable of dehaze and derain, without the need for any additional training.

Recently, OneRestore [25] is proposed to address the challenge of composite degradations, as illustrated in Fig. 2d. OneRestore notably accomplishes the removal of composite degradations in a blind or controllable manner by leveraging visual and textual embeddings. However, it has a significant limitation: it requires training data that encompass all pos-

sible degradations. Given that n isolated degradations can result in $2^n - 1$ distinct degradations, training on the full spectrum becomes increasingly impractical and unreliable as n grows large, due to the substantial training costs and the constraints of model capacity.

In numerous practical scenarios, complexity is often a result of interacting simpler elements. Take the long jump as an example; it primarily involves running and jumping. Similarly, we suspect that managing complex image degradations could be broken down into handling their individual components, thus multi-task models that are trained on several degradations should be able to clear complex degradations that are constituted by these components without further training, as depicted in Fig. 3. Holding this viewpoint, we firstly define a new image restoration task setting, named Universal Image Restoration (UIR). In UIR, the model is trained exclusively on a set of degradation bases and tested on both isolated and composite degradations in a zero-shot manner, as shown in Fig. 2e. Subsequently, we try to feed degraded images that exhibit composite degradations into pre-trained multi-task image restoration models. The intriguing discovery is that all these multi-task models predominantly tackle only one degradation at a time when faced with multiple degradations.

Leveraging this property and drawing inspiration from Chain-of-Thought (CoT) [32, 61], which enables Large Language Models (LLMs) to tackle problems step-by-step, we introduce the Chain of Restoration (CoR). This straightforward yet effective method involves integrating a Degradation Discriminator into a pre-trained multi-task model to identify the degradation status of the input image. Consequently, we can apply the model iteratively in a step-by-step manner, with each step dedicated to the removal of one specific degradation, ultimately restoring the image progressively, shown in Fig. 1. By integrating CoR with existing image

restoration methods, we have successfully achieved UIR. To further facilitate research in this domain, we introduce the first dataset specifically designed for UIR, named the Universal Image Restoration Dataset (UIRD-12). Our main contributions can be encapsulated as follows:

- We introduce a novel task setting for image restoration, *i.e.* Universal Image Restoration (UIR). Within this framework, models are restricted to training on a set of degradation bases and are challenged to handle both individual and composite degradations derived from these bases. Then we present the first dataset designed for UIR, *i.e.* Universal Image Restoration Dataset (UIRD-12). This dataset is comprised of a training set with 5 distinct degradation types and a test set that encompasses 12 different isolated and composite degradation types.
- We introduce the first method for UIR, the Chain of Restoration (CoR). By incorporating a simple Degradation Discriminator, CoR transforms a multi-task model into a universal image restoration model in a zero-shot manner, requiring no additional training.
- Our comprehensive experiments demonstrate the robust capability of CoR. It notably enhances the performance of multi-task models on UIR tasks, often matching or even surpassing SoTA models trained on all the degradations.

2. Related Works

Image Restoration for Composite Degradations. While One-to-One and One-to-Many models address specific degradations, recent research has shifted focus towards composite degradation removal. OneRestore [25] pioneers an unified model leveraging visual and textual embeddings to confront the challenge of composite degradation removal. Nonetheless, it requires comprehensive training data across all degradation types, resulting in high costs and being limited by the model’s capacity. Uniprocessor [19] and RestoreAgent [5] both identify step-by-step removal of composite degradation as feasible for their specialized models. However, [19] only mentions this without further investigation. Moreover, [5] necessitates individual model training for each degradation type and intensity, followed by extra fine-tuning of a large vision-text model for every possible sequence permutation of isolated degradations, rendering the approach prohibitively expensive and impractical. In contrast, our CoR, with a single pre-trained multi-task model, necessitates merely a simple and cheap Degradation Discriminator for step-by-step composite degradation removal, proving its simplicity and efficacy, and demonstrating that any single multi-task model possesses the generalization capability to remove composite degradations in a zero-shot manner. Considering the constraints of previous task settings involving composite degradation, we also introduce Universal Image Restoration (UIR), a task setting where models are trained on a set of degradation bases and evaluated on their ability

Algorithm 1 Pseudocode of CoR in a PyTorch-like style.

```
# X: input image with unknown composite degradation
# M: Multi-task model trained on degradation bases
# cls: The image classifier to discriminate degradations
# ep_o: Soft margin of order, a positive float
# orders: The orders of corresponding bases, a list of integers
# ep_bs: The soft margins of corresponding bases, a list of floats
# n: the number of bases

def Degradation_Discriminator(X, cls, ep_o, orders, ep_b):
    v = cls(X)
    for idx in range(len(orders)):
        # up date v via Eq.(6)
        v[idx] += ep_o * orders[idx] + ep_bs[idx]
    return v.argmax(dim=-1)

def Chain_of_Restoration(X, M, cls, n, ep_o, orders, ep_b):
    type = Degradation_Discriminator(X, cls, ep_o, orders, ep_b) # the
    # degradation situation of I
    while type != n+1: # the image is not clean yet
        X = M(X, type) # a single step
        type = Degradation_Discriminator(X, cls, ep_o, orders, ep_b) #
        # update the degradation situation
    return X # Restored image
```

to remove both individual and composite degradations.

Zero-Shot Learning Zero-shot learning is a paradigm in which machine learning models perform tasks on new data without prior training on similar examples [50]. The rise of Large Language Models (LLMs) and prompting techniques [2, 17, 38, 39, 47] has intensified interest in zero-shot learning within the LLM domain [21, 28, 32, 71]. Specifically, Zero-Shot CoT [32] shows that guiding LLMs to reason step by step significantly improves their performance on complex problems. Motivated by this, we view composite degradations as a sum of several base degradations and propose an iterative method to sequentially remove each type of degradation, progressively restoring the image.

3. Method

3.1. Chain of Restoration

As previously introduced, we observed that multi-task models trained on multiple degradations typically address only one degradation when faced with an image containing composite degradations. Our proposed Chain of Restoration (CoR) capitalizes on this behavior. For an input image \mathbf{X}_0 with composite degradation comprising T components and a multi-task model \mathbf{M} trained on these components, CoR operates step-by-step as follows:

$$\begin{aligned} \text{type} &= \text{Degradation Discriminator}(\mathbf{X}_{i-1}), \\ \mathbf{X}_i &= \mathbf{M}(\mathbf{X}_{i-1}, \text{type}), \quad i = 1, 2, \dots, T \end{aligned} \quad (1)$$

Here, **type** represents the degradation type identified from \mathbf{X}_{i-1} by the Degradation Discriminator. Ideally, the model remove one degradation per step, and after T steps, outputs a clearly restored image \mathbf{X}_T with the degradations removed.

3.2. Degradation Basis

The essence of CoR is the progressive elimination of composite degradations by addressing their individual components.

Models are trained to remove these elemental components, and each of these components is defined as a degradation basis. (Degradation basis essentially refers to an individual degradation.) An n -order degradation refers to a scenario where n isolated degradations are present simultaneously. For example, "rain" and "haze" are termed 1-order bases, while combinations such as "rain+haze" and "haze+snow" are referred to as 2-order bases. Accordingly, we define n -order models as those trained on all the given degradation bases whose order $\leq n$.

To effectively apply CoR for the removal of a specific degradation $d = s_1 + s_2 + \dots + s_m$, where each s_i represents an isolated degradation, it is crucial that the model has been trained on bases b_1, b_2, \dots, b_n that can be directly combined to form d . Given degradation bases The combination of degradation bases is articulated as follows:

$$\text{combine}(b_1, b_2) = b_1 + "+" + b_2 \quad (2)$$

where b_1 , b_2 , and "+" are treated as strings, and + denotes string concatenation. For instance,

$$\text{combine}(\text{haze+snow}, \text{noise}) = \text{haze+snow+noise}.$$

We define the equality of two degradations d_1 and d_2 if one is a permutation of the other:

$$d_1 = d_2 \Leftrightarrow d_1 \in \text{Permu}(d_2) \Leftrightarrow d_2 \in \text{Permu}(d_1) \quad (3)$$

where for a degradation $d = s_1 + s_2 + \dots + s_n$, the permutation set $\text{Permu}(d)$ is:

$$\text{Permu}(d) = \{s_{k_1} + s_{k_2} + \dots + s_{k_n} \mid k_1, k_2, \dots, k_n \text{ is a permutation of } 1, 2, \dots, n\} \quad (4)$$

Determining how multiple bases b_1, b_2, \dots can combine into a degradation d , while maximizing the order of the bases, is computationally complex (NP-hard). What's more, the type of degradation in an input image is often unknown, necessitating a Degradation Discriminator to identify it.

3.3. Degradation Discriminator

To ascertain the degradation state of an input image, a Degradation Discriminator (DD) is essential. Specifically, with a multi-task image restoration model pre-trained on degradation bases b_1, b_2, \dots, b_n , the DD operates in two scenarios:

(1) The given model is blind. In the case of a blind multi-task image restoration model, (like All-in-One models), DD serves to only identify if the input image is clean or degraded. This DD is trained on clean images as well as those with any degradation among b_1, b_2, \dots, b_n , effectively acting as a binary classifier. Specifically, if DD outputs "clean", the iterative process of CoR will stop and return the restored image, otherwise it continues.

(2) The given model is non-blind. For non-blind multi-task image restoration models, (like multi-head/tail methods), the DD must recognize the specific type of degradation present. So this DD is a multiple classifier, designed to differentiate between clean images and those with one of degradations bases b_1, b_2, \dots, b_n . Two challenges persist: (I) The identified degradation type may not be unique, e.g., an image with "haze+rain" could correctly be labeled as "rain," "haze," or "haze+rain." We aim to address higher-order degradations first to optimize performance. (II) The restoration sequence of the bases is not predetermined or controllable, which can impact the outcome. To address these issues, pre-defined hyperparameters soft margins ϵ_o and ϵ_{b_i} are introduced. Given an input image \mathbf{X} with an unknown degradation, the DD generates a probabilistic vector $\mathbf{v} \in \mathbb{R}^{n+1}$:

$$\mathbf{v} = \text{Softmax}(\text{DD}(\mathbf{X})) \quad (5)$$

The i -th element \mathbf{v}_i represents the probability of selecting the degradation basis b_i in this step, while the $(n+1)$ -th element corresponds to the probability of the image being in a "clean" state. Given that the order of b_i is o_i , we can derive the revised probabilistic vector $\mathbf{v}' \in \mathbb{R}^n$ as follows:

$$\mathbf{v}'_i = \mathbf{v}_i + o_i * \epsilon_o + \epsilon_{b_i} \quad (6)$$

Here, ϵ_o represents the soft margin for degradation order, a positive value that favors the selection of higher-order bases. Meanwhile, ϵ_{b_i} is the soft margin for the degradation basis b_i , used to give preference to specific degradation bases. The final choice of basis b_t is determined by:

$$t = \arg \max_t \mathbf{v}'_t \quad (7)$$

The pseudocode of the CoR is provided in Algorithm 1

3.4. Method Complexity

Given n isolated degradations s_1, s_2, \dots, s_n and their corresponding combined degradations $\{s_{k_1} + s_{k_2} + \dots + s_{k_m} \mid 1 \leq k_1 < k_2 < \dots < k_m \leq n, 1 \leq m \leq n\}$, we first define $\phi_n(k)$ as follows:

$$\phi_n(k) = \sum_{t=1}^k C_n^t, \text{ where } C_n^t = \frac{n!}{t!(n-t)!}, 1 \leq k \leq n. \quad (8)$$

Here, $\phi_n(k)$ describes the number of bases a k -order model (trained on all given degradations of order $\leq k$) will be trained to, given n isolated degradations. Assuming each degradation has N training pairs, a k -order model will be trained on $\phi_n(k) \times N$ images for each epoch. We then define the training ratio $TR_n(k)$ as:

$$TR_n(k) = \frac{\phi_n(k)}{\phi_n(1)} = \frac{\phi_n(k)}{n}, \quad 1 \leq k \leq n. \quad (9)$$

Here, $TR_n(k)$ indicates the factor by which the training time for a k -order model exceeds that for a corresponding 1-order model, per training epoch. Although $TR_n(k)$ can't simplify to a concise formula, we know the following: (1) $TR_n(1) = 1$. (2) $TR_n(n) = \frac{2^n - 1}{n}$. (3) $TR_n(k + 1) > TR_n(k)$.

Next, we consider the inference time. We start by defining $\varphi_n(k)$ as follows:

$$\varphi_n(k) = \sum_{t=1}^n C_n^t \left\lceil \frac{t}{k} \right\rceil, \quad 1 \leq k \leq n, \quad (10)$$

where $\lceil * \rceil$ denotes the ceiling function. Similarly, we define the inference ratio $IR_n(k)$ as follows:

$$IR_n(k) = \frac{\varphi_n(k)}{\varphi_n(n)} = \frac{\varphi_n(k)}{2^n - 1}, \quad 1 \leq k \leq n. \quad (11)$$

Assuming all degradations have the same probability of occurrence and the model always prioritizes bases with higher orders, on average, the inference time of a k -order model is $IR_n(k)$ times that of an n -order model (i.e., the end-to-end model like [25]). Although $IR_n(k)$ does not have a simple expression, we know that: (1) $IR_n(1) = \frac{n2^{n-1}}{2^n - 1} \approx \frac{n}{2}$. (2) $IR_n(n) = 1$. (3) $IR_n(k + 1) < IR_n(k)$.

Analysis. Eq. (11) and Eq. (9) show that as the order k of a model increases, it tends to gain more training time and less inference time, as shown in Fig. 4. It can be seen that when k increases, $TR_n(k)$ can grow at an exponential rate and $IR_n(k)$ decreases from fast to slow. Still, the addition of inference time when $k = 1$ is acceptable and the addition of training time when $k = n$ is not acceptable. What's more, a higher order doesn't mean better performance since the capacity of the models is always limited; too much training data can impair the model's overall performance. Considering these, it's recommended to use a relatively low order model when using CoR.

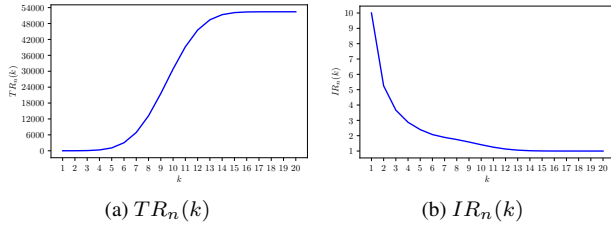


Figure 4. Visualization of $TR_n(k)$ and $IR_n(k)$ when $n = 20$.

4. Experiment

4.1. Experiment Settings

Implementation Details Most results and pre-trained models in this paper are directly from previous works [3, 25, 35, 49]. All the re-trained models (including the image classifiers) are trained with a batch size of 32 (64 for the classifiers)

on 8 NVIDIA GeForce RTX 3090 Ti GPUs. The network optimization is guided by an L_1 loss function, employing the AdamW optimizer [41] with parameters $\beta_1 = 0.9$ and $\beta_2 = 0.999$. The learning rate is set to $2e - 4$ ($2e - 3$ for the classifiers). To enhance the training data, input patches of size 128×128 are utilized, with random horizontal and vertical flips applied to the images to augment the dataset. All the classifiers in this paper are MobileNetV3 small [29].

4.1.1 Datasets

The Synthesised Dataset UIRD-12. We propose a new dataset for UIR, i.e. Universal Image Restoration Dataset-12 (UIRD-12). The training set of UIRD-12 closely follows previous All-in-One works [35, 49]: BSD400 [1] and WED [43] datasets for training on Gaussian denoising ($\sigma = \{15, 25, 50\}$); Rain100L dataset [64] for derain; SOTS dataset [34] for dehaze. For the test set, we use BSD68 [45], Urban100 [30], Rain100L [64], SOTS [34] to synthesise 12 categories of image degradations and their clear counterparts. These degradations include $n1, n2, n5, r, h, h+r, h+n1, h+n5, r+n1, r+n5, h+r+n1, h+r+n5$. ($n1$: noise($\sigma = 15$), $n2$: noise($\sigma = 25$), $n5$: noise($\sigma = 50$), r : rain, h : haze.) Each category contains 100 images. All models are trained on the 5 isolated degradations and tested on the 12 degradations.

Datasets Settings. To better verify the effect of CoR, we utilize not only the UIRD-12 dataset in our experiments but also the CDD-11 dataset [25], which encompasses 11 degradation types including $l, h, r, s, l+h, l+r, l+s, h+r, h+s, l+h+r$, and $l+h+s$. (l : low-light, s : snow, r : rain, h : haze.) Unlike UIRD-12, CDD-11 contains all the corresponding training and testing data for each degradation type. Specifically, 1-order models are trained only on 1-order degradations (i.e. l, h, r, s), 2-order models are trained on all degradations except $l+h+r$ and $l+h+s$, and 3-order models are end-to-end models trained on all degradations.

Compared Methods and Evaluation Metrics. To validate the effectiveness of our proposed CoR, we experiment it with a range of methods. In the experiment on UIRD-12, we primarily select 4 One-to-Many methods including AirNet [35], PromptIR [49], InstructIR [14], HAIR [3], and a One-to-Composite method OneRestore [25]. We combine these methods with CoR to demonstrate its effectiveness. In the experiment on CDD-11, we compare low-order methods integrated with CoR against end-to-end methods, comprising 9 One-to-One image restoration methods (MIRNet [65], MPRNet [66], MIRNetv2 [68], Restormer [67], DGUNet [46], NAFNet [6], SRUDC [53], Fourmer [73], OKNet [15]) and 6 One-to-Many image restoration methods (AirNet [35], TransWeather [56], WeatherDiff [48], PromptIR [49], WGWSNet [75], HAIR [3], and the One-to-Composite method OneRestore [25]). Notably, some methods are trained on different orders. Additionally, we employ the Peak Signal-to-

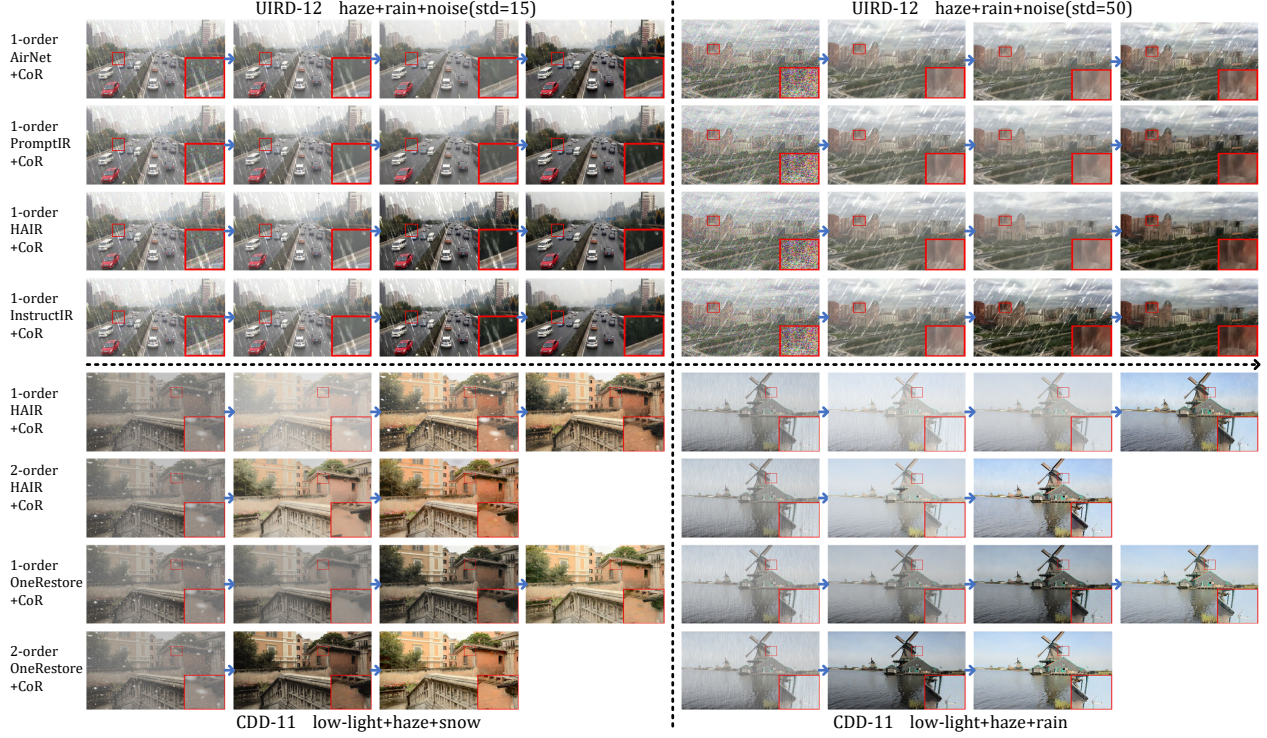


Figure 5. The visualization of the process of CoR with different methods on UIRD-12 and CDD-11.

Noise Ratio (PSNR) and Structure Similarity Index Measure (SSIM) as our evaluation metrics.

4.2. Results

Results on UIRD-12 The results of all the methods on UIRD-12 are presented in Tab. 1 and Fig. 6. It's obvious that our proposed CoR can significantly improve the performance of these 1-order multi-task models on composite degradation removal with only the addition of a simple Degradation Discriminator, while having nearly no impact on isolated degradation removal. What's more, we find that non-blind models gain obviously more increment from CoR than blind models. This is because non-blind methods know the exact degradation type they are processing, thus alleviating the Degradation Coupling issue described in Sec. 5. The results show the effectiveness and feasibility of CoR.

Results on CDD-11 The results of all the methods on CDD-11 are presented in Tab. 2 and Fig. 7. It can be seen that with CoR, models with low orders can achieve comparable or even superior performance to models trained on all degradations. Notably, the 2-order OneRestore with CoR achieves comparable performance with the 3-order OneRestore, and the 2-order HAIR with CoR surpasses the 3-order HAIR in both PSNR and SSIM, demonstrating the effectiveness of CoR. As previously discussed, due to limited capacity, training the model on all degradations can lead to decreased performance on each degradation, which is why

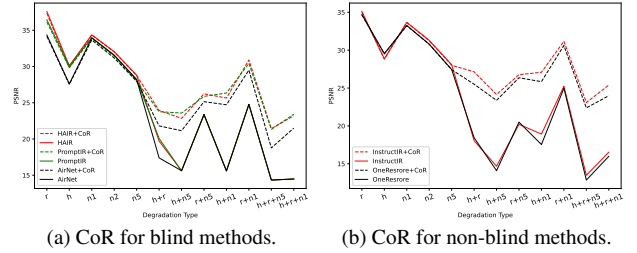


Figure 6. Visual Comparison of Multi-Task Models' Performance with and without CoR on UIRD-12.

2-order methods with CoR can perform better with less training. However, as shown in Fig. 7, 1-order HAIR with CoR fail to achieve satisfactory results in composite degradations with low-light due to the Degradation Coupling described in Sec. 5. Additionally, we provide a training time comparison in Tab. 3. It is evident that models with lower orders require less time and thus have lower training costs to converge, not only due to the reduced time cost per epoch but also because less data requires fewer epochs to converge.

Visual Results We present visual results in Fig. 5 and Fig. 8. Fig. 5 illustrates how CoR assists multi-task models in step-by-step removal of composite degradations. It is evident that each step typically addresses only one degradation basis that the models are trained on, which is a common

Table 1. Average quantitative performance comparison on the UIRD-12 dataset. "+CoR" indicates the direct integration of the pre-trained model with CoR, while "+1.52M" signifies that CoR introduces only an additional 1.52 M parameters.

Types	Methods	Order	Blind	PSNR \uparrow	SSIM \uparrow	#Params
-	Input	-	-	17.19	0.4523	-
One-to-Many	AirNet [35]	1	✓	23.44	0.7902	8.93M
	PromptIR [49]	1	✓	24.03	0.7904	35.59M
	InstructIR [14]	1	✗	23.68	0.7042	15.94M
	HAIR [3]	1	✓	24.23	0.7939	28.56M
One-to-Composite	OneRestore [†] [25]	1	✗	23.34	0.6952	5.98M
One-to-Universal	AirNet[35]+CoR	1	✓	26.43	0.8407	+1.52M
	PromptIR[49]+CoR	1	✓	27.83	0.8556	
	InstructIR[14]+CoR	1	✓	28.44	0.8726	
	HAIR[3]+CoR	1	✓	28.04	0.8664	
	OneRestore [†] [25]+CoR	1	✓	27.78	0.8607	

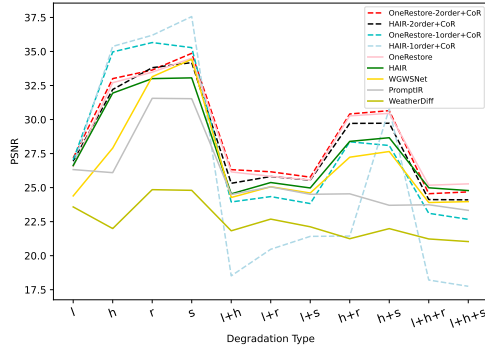


Figure 7. Visualization of performance of multi-task models on CDD-12. Methods without "order" are all 3-order end-to-end models trained on all degradations.

observation. Furthermore, it is also noticeable that models with higher orders require fewer steps to restore the image, consistent with our discussion in Sec. 3.4. Fig. 8 displays the visual comparison of various methods on CDD-11. It is apparent that methods integrated with CoR exhibit comparable, or even superior, visual performance compared to end-to-end methods. Notably, even the 1-order OneRestore achieves satisfactory performance with CoR. However, it is also evident that the 1-order HAIR performs poorly due to Degradation Coupling, as detailed in Sec. 5.

4.3. Ablation Study

Ablation Study of Degradation Discriminator. As shown in Tab. 4, we investigate the influence of the proposed Degradation Discriminator across five distinct settings: (a) Without the Degradation Discriminator, the model randomly selects a degradation basis or halts the restoration upon receiving an input. (b) A pristine classifier is employed each time to determine the degradation basis or to decide when to stop the restoration process. (c) The model incorporates ϵ_o . (d) The model incorporates ϵ_{b_i} . (e) The model utilizes both ϵ_o

Table 2. Comparison of average quantitative results on the CDD-11 dataset. "+CoR" indicates the direct integration of the pre-trained model with CoR. Red and blue represent the best and second-best results, respectively.

Types	Methods	Order	Blind	PSNR \uparrow	SSIM \uparrow	#Params
-	Input	-	-	16.00	0.6008	-
One-to-One	MIRNet [65]	3	✓	25.97	0.8474	31.79M
	MPRNet [66]	3	✓	25.47	0.8555	15.74M
	MIRNetv2 [68]	3	✓	25.37	0.8335	5.86M
	Restormer [67]	3	✓	26.99	0.8646	26.13M
	DGUNet [46]	3	✓	26.92	0.8559	17.33M
	NAFNet [6]	3	✓	24.13	0.7964	17.11M
	SRUDC [53]	3	✓	27.64	0.8600	6.80M
	Fourmer [73]	3	✓	23.44	0.7885	0.55M
	OKNet [15]	3	✓	26.33	0.8605	4.72M
	AirNet [35]	3	✓	23.75	0.8140	8.93M
One-to-Many	TransWeather [56]	3	✓	23.13	0.7810	21.90M
	WeatherDiff [48]	3	✓	22.49	0.7985	82.96M
	PromptIR [49]	3	✓	25.90	0.8499	38.45M
	WGWSNet [75]	3	✗	26.96	0.8626	25.76M
	HAIR [3]	1	✓	23.01	0.7632	28.56M
	HAIR [3]	2	✓	27.65	0.8655	28.56M
	HAIR [3]	3	✓	27.85	0.8663	28.56M
	HAIR [3]	3	✓	27.85	0.8663	28.56M
One-to-Composite	OneRestore [25]	1	✗	21.43	0.7226	5.98M
	OneRestore [25]	2	✗	27.28	0.8437	5.98M
	OneRestore [25]	3	✗	28.72	0.8821	5.98M
One-to-Universal	HAIR[3]+CoR	1	✓	25.85	0.8289	+1.52M
	HAIR[3]+CoR	2	✓	28.33	0.8688	
	OneRestore [†] [25]+CoR	1	✓	27.94	0.8541	
	OneRestore [†] [25]+CoR	2	✓	28.84	0.8794	

Table 3. Comprison of training time. Results are from CDD-11 on 8 NVIDIA GeForce RTX 3090 Ti GPUs, we re-train all the methods until convergence (including the training of Classifier).

Method	HAIR	HAIR	HAIR	OneRestore	OneRestore	OneRestore
Order	1	2	3	1	2	3
Time	30.71h	76.25h	109.76h	21.39h	53.62h	71.70h

and ϵ_{b_i} . The significance of ϵ_o is evident in its ability to prioritize degradation bases of higher orders. Similarly, ϵ_{b_i} underscores the value of selecting an appropriate restoration sequence, as illustrated in Fig. 9. Collectively, these findings validate the rationale behind our design of the Degradation Discriminator.

Table 4. Impact of key components Degradation Discriminator. Results are from low-light+haze+snow task on CDD-11 using a pre-trained 2-order OneRestore model.

Setting	Classifier	ϵ_o	ϵ_{b_i}	PSNR	SSIM
(a)	✗	✗	✗	15.02	0.5137
(b)	✓	✗	✗	19.69	0.7109
(c)	✓	✓	✗	21.15	0.7388
(d)	✓	✗	✓	22.36	0.7482
(e) (ours)	✓	✓	✓	24.68	0.7558

Effect of Bases. As discussed in Sec. 3, a fundamental assumption of CoR is that the composite degradations encountered must be directly combinable from the bases on

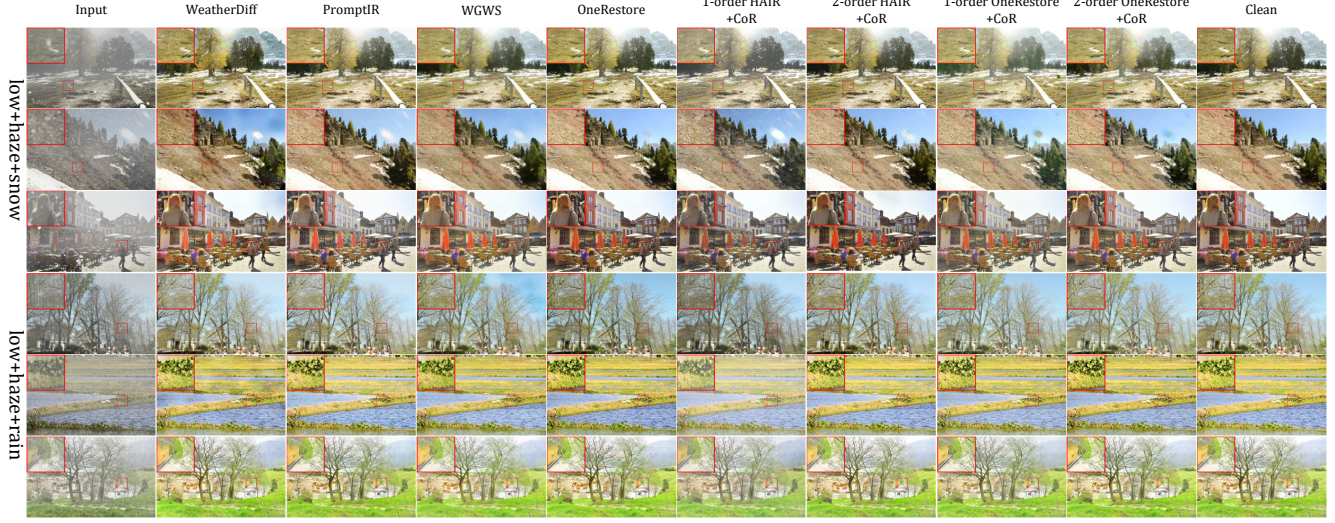


Figure 8. Visual comparison on CDD-11.

which the models are trained. This concept is validated in Tab. 5. In setting (a), the input images cannot be restored because the selected bases lack the "low" component. Setting (b) includes "low," "haze," and "rain," but the combinations "rain+haze" and "low+haze" cannot be directly merged into "low+haze+rain," resulting in suboptimal outcomes. Both settings (c) and (d) perform well, with (d) showing superior performance due to the inclusion of higher-order degradation bases. Selecting appropriate degradation bases is crucial for effective restoration.

Table 5. Performance of the OneRestore trained under different bases with CoR on low+haze+rain of CDD-11.

Setting	low	rain	haze	rain+haze	low+haze	PSNR	SSIM
(a)	✗	✓	✓	✓	✗	14.37	0.5259
(b)	✗	✗	✗	✓	✓	20.03	0.7031
(c)	✓	✓	✓	✗	✗	22.87	0.7564
(d)	✓	✓	✓	✓	✓	24.57	0.7699

5. Limitation & Future Prospect

Before delving into the limitations, it is crucial to define a key concept: **Degradation Coupling**. Consider input images $x \sim p(x|s_1, s_2, \dots, s_n)$, where $p(x|s_1, s_2, \dots, s_n)$ represents the distribution of images subjected to composite degradations $s_1 + s_2 + \dots + s_n$. Let \mathbf{M} be a model trained on degradation bases b_1, b_2, \dots, b_m . Suppose that $s_1 + s_2 + \dots + s_n$ can be expressed as $b_{k_1} + b_{k_2} + \dots + b_{k_t}$, and the model \mathbf{M} sequentially removes these degradations starting with b_{k_1} . If the following condition holds:

$$p(x|\mathbf{M}[b_{k_1}], b_{k_2}, \dots, b_{k_t}) \neq p(x|b_{k_2}, \dots, b_{k_t}) \quad (12)$$

we term this phenomenon **Degradation Coupling**. Here, $\mathbf{M}[b_{k_1}]$ indicates that the model \mathbf{M} has been applied to eliminate the degradation b_{k_1} from x . In essence, Degradation

Coupling occurs when the model's removal of one degradation inadvertently affects other unintended degradations. This issue arises because the model wasn't trained to handle the scenario where $p(x|\mathbf{M}[b_{k_1}], b_{k_2}, \dots, b_{k_t})$. For example, as depicted in Fig. 9, when the model first attempts to remove low-light conditions, it inadvertently enhances other degradations like snow and haze, which it hasn't learned to address. Conversely, if the model first removes snow, which affects other degradations less, it can then more effectively restore the image. Tables 1 and 2 show CoR performs better with non-blind methods, which can control the removal of one degradation at a time, thus reducing Degradation Coupling. Therefore, CoR is more suitable for non-blind methods.

Given the inherent interdependencies among degradations in composite degradations, Degradation Coupling is an unavoidable issue. While adjusting the restoration sequence may offer some relief, its effectiveness is limited. The direction of future works should be to develop strategies that (1) enable the model to clearly remove the targeted degradation b_i , and (2) minimize the impact on other degradations. We look forward to future work that can develop algorithms to more effectively address this limitation.

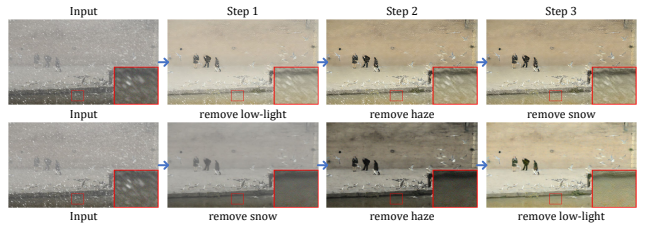


Figure 9. The visualization of the process of CoR in different restoration sequence using the same pre-trained OneRestore model.

6. Conclusion

In this paper, we introduce a new task setting called Universal Image Restoration (UIR) to address the limitations of previous settings. UIR challenges the model to be trained on a set of degradation bases and then tested on images with isolated or composite degradations in a zero-shot manner. To meet this challenge, we propose the first algorithm for UIR, known as Chain-of-Restoration (CoR). CoR enhances a pre-trained multi-task model with a Degradation Discriminator, enabling it to remove one degradation basis at a time and restore degraded images step by step. Our extensive experiments indicate that CoR significantly boosts model performance in removing composite degradations, rivaling or even outperforming end-to-end methods trained on all degradations, as demonstrated by both quantitative and visual results. Lastly, we discuss the limitations and future prospects of CoR. We are confident that this work will offer new insights to the research community.

References

- [1] Pablo Arbelaez, Michael Maire, Charless Fowlkes, and Jitendra Malik. Contour detection and hierarchical image segmentation. *IEEE TPAMI*, 33(5):898–916, 2010. 5
- [2] Tom Brown, Benjamin Mann, Nick Ryder, Melanie Subbiah, Jared D Kaplan, Prafulla Dhariwal, Arvind Neelakantan, Pranav Shyam, Girish Sastry, Amanda Askell, Sandhini Agarwal, Ariel Herbert-Voss, Gretchen Krueger, Tom Henighan, Rewon Child, Aditya Ramesh, Daniel Ziegler, Jeffrey Wu, Clemens Winter, Chris Hesse, Mark Chen, Eric Sigler, Mateusz Litwin, Scott Gray, Benjamin Chess, Jack Clark, Christopher Berner, Sam McCandlish, Alec Radford, Ilya Sutskever, and Dario Amodei. Language models are few-shot learners. In *NeurIPS*, pages 1877–1901. Curran Associates, Inc., 2020. 3
- [3] Jin Cao, Yi Cao, Li Pang, Deyu Meng, and Xiangyong Cao. Hair: Hypernetworks-based all-in-one image restoration, 2024. 2, 5, 7
- [4] Hanting Chen, Yunhe Wang, Tianyu Guo, Chang Xu, Yiping Deng, Zhenhua Liu, Siwei Ma, Chunjing Xu, Chao Xu, and Wen Gao. Pre-trained image processing transformer. In *CVPR*, pages 12299–12310, 2021. 2
- [5] Haoyu Chen, Wenbo Li, Jinjin Gu, Jingjing Ren, Sixiang Chen, Tian Ye, Renjing Pei, Kaiwen Zhou, Fenglong Song, and Lei Zhu. Restoreagent: Autonomous image restoration agent via multimodal large language models, 2024. 3
- [6] Liangyu Chen, Xiaojie Chu, Xiangyu Zhang, and Jian Sun. Simple baselines for image restoration. In *ECCV*, pages 17–33. Springer, 2022. 1, 5, 7
- [7] Sixiang Chen, Tian Ye, Yun Liu, Taodong Liao, Jingxia Jiang, Erkang Chen, and Peng Chen. Msp-former: Multi-scale projection transformer for single image desnowing. In *ICASSP*, pages 1–5, 2023. 1
- [8] Wei-Ting Chen, Zhi-Kai Huang, Cheng-Che Tsai, Hao-Hsiang Yang, Jian-Jiun Ding, and Sy-Yen Kuo. Learning multiple adverse weather removal via two-stage knowledge learning and multi-contrastive regularization: Toward a unified model. In *CVPR*, pages 17653–17662, 2022. 1, 2
- [9] Xiang Chen, Hao Li, Mingqiang Li, and Jinshan Pan. Learning a sparse transformer network for effective image deraining. In *CVPR*, pages 5896–5905, 2023. 1
- [10] Xiangyu Chen, Xintao Wang, Jiantao Zhou, Yu Qiao, and Chao Dong. Activating more pixels in image super-resolution transformer. In *CVPR*, pages 22367–22377, 2023. 1
- [11] Zheng Chen, Yulun Zhang, Jinjin Gu, Linghe Kong, Xin Yuan, et al. Cross aggregation transformer for image restoration. *NeurIPS*, 35:25478–25490, 2022. 1
- [12] Zheng Chen, Yiwen Sun, Xiaojun Bi, and Jianyu Yue. Lightweight image de-snowing: A better trade-off between network capacity and performance. *Neural Networks*, 165: 896–908, 2023. 1
- [13] Zheng Chen, Yulun Zhang, Jinjin Gu, Linghe Kong, Xiaokang Yang, and Fisher Yu. Dual aggregation transformer for image super-resolution. In *CVPR*, pages 12312–12321, 2023. 1
- [14] Marcos V Conde, Gregor Geigle, and Radu Timofte. Instructir: High-quality image restoration following human instructions. In *ECCV*, 2024. 5, 7

- [15] Yuning Cui, Wenqi Ren, and Alois Knoll. Omni-kernel network for image restoration. In *AAAI*, pages 1426–1434, 2024. 5, 7
- [16] Kostadin Dabov, Alessandro Foi, Vladimir Katkovnik, and Karen Egiazarian. Color image denoising via sparse 3d collaborative filtering with grouping constraint in luminance-chrominance space. In *2007 IEEE International Conference on Image Processing*, pages I–313. IEEE, 2007. 1
- [17] Jacob Devlin, Ming-Wei Chang, Kenton Lee, and Kristina Toutanova. BERT: Pre-training of deep bidirectional transformers for language understanding. In *NAACL*, pages 4171–4186, 2019. 3
- [18] Yong Du, Junjie Deng, Yulong Zheng, Junyu Dong, and Shengfeng He. Dsdnet: Toward single image deraining with self-paced curricular dual stimulations. *CVIU*, 230:103657, 2023. 1
- [19] Huiyu Duan, Xiongkuo Min, Sijing Wu, Wei Shen, and Guangtao Zhai. Uniprocessor: A text-induced unified low-level image processor. In *ECCV*, 2024. 3
- [20] Xueyang Fu, Jie Xiao, Yurui Zhu, Aiping Liu, Feng Wu, and Zheng-Jun Zha. Continual image deraining with hypergraph convolutional networks. *IEEE TPAMI*, 45(8):9534–9551, 2023. 1
- [21] Nate Gruver, Marc Finzi, Shikai Qiu, and Andrew G Wilson. Large language models are zero-shot time series forecasters. In *NeurIPS*, pages 19622–19635. Curran Associates, Inc., 2023. 3
- [22] Chun-Le Guo, Qixin Yan, Saeed Anwar, Runmin Cong, Wenqi Ren, and Chongyi Li. Image dehazing transformer with transmission-aware 3d position embedding. In *CVPR*, pages 5812–5820, 2022. 1
- [23] Hang Guo, Jinmin Li, Tao Dai, Zhihao Ouyang, Xudong Ren, and Shu-Tao Xia. Mambair: A simple baseline for image restoration with state-space model. In *ECCV*, 2024. 1
- [24] Xiaojie Guo and Qiming Hu. Low-light image enhancement via breaking down the darkness. *IJCV*, 131(1):48–66, 2023. 1
- [25] Yu Guo, Yuan Gao, Yuxu Lu, Ryan Wen Liu, and Shengfeng He. Onerestore: A universal restoration framework for composite degradation. In *ECCV*, 2024. 2, 3, 5, 7
- [26] Junlin Han, Weihao Li, Pengfei Fang, Chunyi Sun, Jie Hong, Mohammad Ali Armin, Lars Petersson, and Hongdong Li. Blind image decomposition. In *ECCV*, pages 218–237, 2022. 2
- [27] Trung Hoang, Haichuan Zhang, Amirsaeed Yazdani, and Vishal Monga. Transer: Hybrid model and ensemble-based sequential learning for non-homogenous dehazing. In *CVPR*, pages 1670–1679, 2023. 1
- [28] Yupeng Hou, Junjie Zhang, Zihan Lin, Hongyu Lu, Ruobing Xie, Julian McAuley, and Wayne Xin Zhao. Large language models are zero-shot rankers for recommender systems, 2024. 3
- [29] Andrew Howard, Mark Sandler, Grace Chu, Liang-Chieh Chen, Bo Chen, Mingxing Tan, Weijun Wang, Yukun Zhu, Ruoming Pang, Vijay Vasudevan, Quoc V. Le, and Hartwig Adam. Searching for mobilenetv3. In *ICCV*, 2019. 5
- [30] Jia-Bin Huang, Abhishek Singh, and Narendra Ahuja. Single image super-resolution from transformed self-exemplars. In *CVPR*, pages 5197–5206, 2015. 5
- [31] Kui Jiang, Zhongyuan Wang, Peng Yi, Chen Chen, Baojin Huang, Yimin Luo, Jiayi Ma, and Junjun Jiang. Multi-scale progressive fusion network for single image deraining. In *CVPR*, pages 8346–8355, 2020. 1
- [32] Takeshi Kojima, Shixiang (Shane) Gu, Machel Reid, Yutaka Matsuo, and Yusuke Iwasawa. Large language models are zero-shot reasoners. In *NeurIPS*, pages 22199–22213, 2022. 2, 3
- [33] Jaakko Lehtinen, Jacob Munkberg, Jon Hasselgren, Samuli Laine, Tero Karras, Miika Aittala, and Timo Aila. Noise2noise: Learning image restoration without clean data. *ICML*, 2018. 1
- [34] Boyi Li, Wenqi Ren, Dengpan Fu, Dacheng Tao, Dan Feng, Wenjun Zeng, and Zhangyang Wang. Benchmarking single-image dehazing and beyond. *IEEE TIP*, 28(1):492–505, 2018. 5
- [35] Boyun Li, Xiao Liu, Peng Hu, Zhongqin Wu, Jiancheng Lv, and Xi Peng. All-in-one image restoration for unknown corruption. In *CVPR*, pages 17452–17462, 2022. 2, 5, 7
- [36] Ruoteng Li, Robby T Tan, and Loong-Fah Cheong. All in one bad weather removal using architectural search. In *CVPR*, pages 3175–3185, 2020. 1, 2
- [37] Jingyun Liang, Jiezhong Cao, Guolei Sun, Kai Zhang, Luc Van Gool, and Radu Timofte. Swinir: Image restoration using swin transformer. In *CVPR*, pages 1833–1844, 2021. 1
- [38] Jiachang Liu, Dinghan Shen, Yizhe Zhang, Bill Dolan, Lawrence Carin, and Weizhu Chen. What makes good in-context examples for gpt-3? *arXiv preprint arXiv:2101.06804*, 2021. 3
- [39] Pengfei Liu, Weizhe Yuan, Jinlan Fu, Zhengbao Jiang, Hiroaki Hayashi, and Graham Neubig. Pre-train, prompt, and predict: A systematic survey of prompting methods in natural language processing. *arXiv preprint arXiv:2107.13586*, 2021. 3
- [40] Risheng Liu, Long Ma, Jiaao Zhang, Xin Fan, and Zhongxuan Luo. Retinex-inspired unrolling with cooperative prior architecture search for low-light image enhancement. In *CVPR*, pages 10561–10570, 2021. 1
- [41] Ilya Loshchilov, Frank Hutter, et al. Fixing weight decay regularization in adam. *arXiv preprint arXiv:1711.05101*, 5, 2017. 5
- [42] Yu Luo, Qingdong Huang, Jie Ling, Kailong Lin, and Teng Zhou. Local and global knowledge distillation with direction-enhanced contrastive learning for single-image deraining. *Knowledge-Based Syst.*, 268:110480, 2023. 1
- [43] Kede Ma, Zhengfang Duanmu, Qingbo Wu, Zhou Wang, Hongwei Yong, Hongliang Li, and Lei Zhang. Waterloo exploration database: New challenges for image quality assessment models. *IEEE TIP*, 26(2):1004–1016, 2016. 5
- [44] Salma Abdel Magid, Yulun Zhang, Donglai Wei, Won-Dong Jang, Zudi Lin, Yun Fu, and Hanspeter Pfister. Dynamic high-pass filtering and multi-spectral attention for image super-resolution. In *CVPR*, pages 4288–4297, 2021. 1

- [45] David Martin, Charless Fowlkes, Doron Tal, and Jitendra Malik. A database of human segmented natural images and its application to evaluating segmentation algorithms and measuring ecological statistics. In *ICCV*, 2001. [5](#)
- [46] Chong Mou, Qian Wang, and Jian Zhang. Deep generalized unfolding networks for image restoration. In *CVPR*, pages 17399–17410, 2022. [5](#), [7](#)
- [47] Long Ouyang, Jeff Wu, Xu Jiang, Diogo Almeida, Carroll L. Wainwright, Pamela Mishkin, Chong Zhang, Sandhini Agarwal, Katarina Slama, Alex Ray, John Schulman, Jacob Hilton, Fraser Kelton, Luke Miller, Maddie Simens, Amanda Askell, Peter Welinder, Paul Christiano, Jan Leike, and Ryan Lowe. Training language models to follow instructions with human feedback, 2022. [3](#)
- [48] Ozan Özdenizci and Robert Legenstein. Restoring vision in adverse weather conditions with patch-based denoising diffusion models. *IEEE TPAMI*, 45(8):10346–10357, 2023. [2](#), [5](#), [7](#)
- [49] Vaishnav Potlapalli, Syed Waqas Zamir, Salman H Khan, and Fahad Shahbaz Khan. PromptIR: Prompting for all-in-one image restoration. *NeurIPS*, 36, 2024. [2](#), [5](#), [7](#)
- [50] Farhad Pourpanah, Moloud Abdar, Yuxuan Luo, Xinlei Zhou, Ran Wang, Chee Peng Lim, Xi-Zhao Wang, and Q. M. Jonathan Wu. A review of generalized zero-shot learning methods. *IEEE TPAMI*, 45(4):4051–4070, 2023. [3](#)
- [51] Yanyun Qu, Yizi Chen, Jingying Huang, and Yuan Xie. Enhanced pix2pix dehazing network. In *CVPR*, pages 8160–8168, 2019. [1](#)
- [52] Yuhui Quan, Xiaoheng Tan, Yan Huang, Yong Xu, and Hui Ji. Image desnowing via deep invertible separation. *IEEE TCSVT*, 33(7):3133–3144, 2023. [1](#)
- [53] Binbin Song, Xiangyu Chen, Shuning Xu, and Jiantao Zhou. Under-display camera image restoration with scattering effect. In *ICCV*, pages 12580–12589, 2023. [5](#), [7](#)
- [54] Yuda Song, Zhuqing He, Hui Qian, and Xin Du. Vision transformers for single image dehazing. *IEEE TIP*, 32:1927–1941, 2023. [1](#)
- [55] Chunwei Tian, Yong Xu, and Wangmeng Zuo. Image denoising using deep cnn with batch renormalization. *Neural Networks*, 2020. [1](#)
- [56] Jeya Maria Jose Valanarasu, Rajeev Yasarla, and Vishal M Patel. Transweather: Transformer-based restoration of images degraded by adverse weather conditions. In *CVPR*, pages 2353–2363, 2022. [2](#), [5](#), [7](#)
- [57] Chao Wang, Zhedong Zheng, Ruijie Quan, Yifan Sun, and Yi Yang. Context-aware pretraining for efficient blind image decomposition. In *CVPR*, pages 18186–18195, 2023. [2](#)
- [58] Tianyu Wang, Xin Yang, Ke Xu, Shaozhe Chen, Qiang Zhang, and Rynson WH Lau. Spatial attentive single-image deraining with a high quality real rain dataset. In *CVPR*, pages 12270–12279, 2019. [1](#)
- [59] Yinglong Wang, Chao Ma, and Jianzhuang Liu. Smartassign: Learning a smart knowledge assignment strategy for deraining and desnowing. In *CVPR*, pages 3677–3686, 2023. [2](#)
- [60] Zhendong Wang, Xiaodong Cun, Jianmin Bao, Wengang Zhou, Jianzhuang Liu, and Houqiang Li. Uformer: A general u-shaped transformer for image restoration. In *CVPR*, pages 17683–17693, 2022. [1](#)
- [61] Jason Wei, Xuezhi Wang, Dale Schuurmans, Maarten Bosma, brian ichter, Fei Xia, Ed Chi, Quoc V Le, and Denny Zhou. Chain-of-thought prompting elicits reasoning in large language models. In *NeurIPS*, pages 24824–24837. Curran Associates, Inc., 2022. [2](#)
- [62] Xiaogang Xu, Ruixing Wang, Chi-Wing Fu, and Jiaya Jia. Snr-aware low-light image enhancement. In *CVPR*, pages 17714–17724, 2022. [1](#)
- [63] Xiaogang Xu, Ruixing Wang, and Jiangbo Lu. Low-light image enhancement via structure modeling and guidance. In *CVPR*, pages 9893–9903, 2023. [1](#)
- [64] Fuzhi Yang, Huan Yang, Jianlong Fu, Hongtao Lu, and Bain-ing Guo. Learning texture transformer network for image super-resolution. In *CVPR*, 2020. [5](#)
- [65] Syed Waqas Zamir, Aditya Arora, Salman Khan, Munawar Hayat, Fahad Shahbaz Khan, Ming-Hsuan Yang, and Ling Shao. Learning enriched features for real image restoration and enhancement. In *ECCV*, pages 492–511, 2020. [5](#), [7](#)
- [66] Syed Waqas Zamir, Aditya Arora, Salman Khan, Munawar Hayat, Fahad Shahbaz Khan, Ming-Hsuan Yang, and Ling Shao. Multi-stage progressive image restoration. In *CVPR*, pages 14821–14831, 2021. [1](#), [5](#), [7](#)
- [67] Syed Waqas Zamir, Aditya Arora, Salman Khan, Munawar Hayat, Fahad Shahbaz Khan, and Ming-Hsuan Yang. Restormer: Efficient transformer for high-resolution image restoration. In *CVPR*, pages 5728–5739, 2022. [1](#), [5](#), [7](#)
- [68] Syed Waqas Zamir, Aditya Arora, Salman Khan, Munawar Hayat, Fahad Shahbaz Khan, Ming-Hsuan Yang, and Ling Shao. Learning enriched features for fast image restoration and enhancement. *IEEE TPAMI*, 45(2):1934–1948, 2022. [5](#), [7](#)
- [69] Kai Zhang, Wangmeng Zuo, Yunjin Chen, Deyu Meng, and Lei Zhang. Beyond a gaussian denoiser: Residual learning of deep cnn for image denoising. *IEEE TIP*, 26(7):3142–3155, 2017. [1](#)
- [70] Kai Zhang, Wangmeng Zuo, and Lei Zhang. Ffdnet: Toward a fast and flexible solution for cnn-based image denoising. *IEEE TIP*, 27(9):4608–4622, 2018. [1](#)
- [71] Zhuosheng Zhang, Aston Zhang, Mu Li, and Alex Smola. Automatic chain of thought prompting in large language models. In *ICLR*, 2023. [3](#)
- [72] Yu Zheng, Jiahui Zhan, Shengfeng He, Junyu Dong, and Yong Du. Curricular contrastive regularization for physics-aware single image dehazing. In *CVPR*, pages 5785–5794, 2023. [1](#)
- [73] Man Zhou, Jie Huang, Chun-Le Guo, and Chongyi Li. Fourmer: An efficient global modeling paradigm for image restoration. In *ICML*, pages 42589–42601, 2023. [5](#), [7](#)
- [74] Mingliang Zhou, Xingtai Wu, Xuekai Wei, Tao Xiang, Bin Fang, and Sam Kwong. Low-light enhancement method based on a retinex model for structure preservation. *IEEE TMM*, pages 1–13, 2023. [1](#)
- [75] Yurui Zhu, Tianyu Wang, Xueyang Fu, Xuanyu Yang, Xin Guo, Jifeng Dai, Yu Qiao, and Xiaowei Hu. Learning weather-general and weather-specific features for image restoration under multiple adverse weather conditions. In *CVPR*, pages 21747–21758, 2023. [5](#), [7](#)